

Outer radiation belt boundary location relative to the magnetopause: Implications for magnetopause shadowing

C. Matsumura,¹ Y. Miyoshi,¹ K. Seki,¹ S. Saito,^{1,2} V. Angelopoulos,³ and J. Koller⁴

Received 18 February 2011; revised 13 May 2011; accepted 17 May 2011; published 18 June 2011.

[1] Relativistic electron fluxes of the outer radiation belt often decrease rapidly in response to solar wind disturbances. The importance of the magnetopause shadowing (MPS) effect on such electron losses has yet to be quantified. If the MPS is essential for outer radiation belt electron losses, a close relationship between the outer edge of the outer belt and the magnetopause standoff distance is expected. Using GOES and THEMIS data, we examined earthward movement of the outer edge of the outer belt during electron loss events at geosynchronous orbit and its correlation with the magnetopause standoff distance. In events with significant earthward movement, we found a good correlation. There were no clear correlations in events without significant earthward movement, however. Comparing the observational results with a test particle simulation, the observed dependence between the outer edge and the magnetopause standoff distance is consistent with the MPS effect.

Citation: Matsumura, C., Y. Miyoshi, K. Seki, S. Saito, V. Angelopoulos, and J. Koller (2011), Outer radiation belt boundary location relative to the magnetopause: Implications for magnetopause shadowing, *J. Geophys. Res.*, *116*, A06212, doi:10.1029/2011JA016575.

1. Introduction

[2] Relativistic electron flux in the outer radiation belt is highly variable during geomagnetic storms [e.g., *Reeves et al.*, 2003; *Miyoshi and Kataoka*, 2005, 2011]. During the main phase, outer belt electron flux decreases rapidly [e.g., *Nagai*, 1988; *Miyoshi et al.*, 2003]. The flux decrease is in part due to the *Dst* effect, an adiabatic, reversible response to the evolution of the storm time ring current [*Kim and Chan*, 1997]. Since the electron flux does not always return to prestorm levels [e.g., *Onsager et al.*, 2002; *Reeves et al.*, 2003], other loss processes should cause irreversible electron loss. Outer radiation belt electrons also decrease rapidly during nonstorm times, in association with solar wind disturbances [e.g., *Kim et al.*, 2006]. Mechanisms proposed to explain this phenomenon include precipitation into the atmosphere from wave-particle interactions and drift loss through the dayside magnetopause due to both outward diffusion and magnetopause shadowing (MPS).

[3] Several types of plasma waves (whistler hiss, chorus, and electromagnetic ion cyclotron waves (EMIC)) that can cause precipitation loss have been investigated (see *Millan and Thorne* [2007] for a review). Although pitch angle scattering is important for electron loss, the loss sometimes

occurs on time scales faster than those of typical electron lifetimes expected from wave-particle interactions. For example, the typical loss rate from whistler chorus is about 1 day [e.g., *O'Brien et al.*, 2004] and that from whistler hiss waves is on the order of 5–10 days [e.g., *Lyons et al.*, 1972]. Both rates are longer than the rapid loss of electrons observed at the outer portion of the outer belt. EMIC waves can cause rapid loss of relativistic electrons when electron energy becomes relativistic [*Li et al.*, 2007; *Jordanova et al.*, 2008; *Miyoshi et al.*, 2008]. *Borovsky and Denton* [2009] performed a superposed epoch analysis to detect global flux dropouts for 1.1–1.5 MeV at geosynchronous orbit. They showed that EMIC waves are a primary mechanism for electron loss. A number of observations, however, have indicated that although electron losses occur not only at MeV energies but also over a wide energy range [e.g., *Millan and Thorne*, 2007], and EMIC waves are unlikely to resonate with sub-relativistic electrons [*Morley et al.*, 2010].

[4] The MPS is another important electron loss process. If the drift shell of electrons is opened to the magnetopause, electrons are lost permanently from the magnetosphere. *Ohtani et al.* [2009] showed that during loss events at geosynchronous orbit, the solar wind dynamic pressure tends to be high, and the interplanetary magnetic field (IMF) B_z tends to be more southward. Under such conditions, magnetic field intensity at the subsolar magnetopause is usually stronger than at nightside geosynchronous orbit, and relativistic electrons can escape through the dayside magnetopause. *Green et al.* [2004], however, suggested that the MPS cannot explain the flux dropouts because of discrepancies between the magnetopause standoff distance and the electron flux depression region.

¹Solar-Terrestrial Environment Laboratory, Nagoya University, Nagoya, Japan.

²Now at National Institute of Information and Communications Technology, Koganei, Japan.

³IGPP, University of California, Los Angeles, California, USA.

⁴Los Alamos National Laboratory, Los Alamos, New Mexico, USA.

[5] Several test particle simulations assert the importance of the MPS as an electron loss mechanism [Ukhorskiy *et al.*, 2006; Kim *et al.*, 2008, 2010; Saito *et al.*, 2010]. Using a two-dimensional test particle simulation, Ukhorskiy *et al.* [2006] showed that the MPS is important for electron loss through drift orbit expansion by ring current evolution. Kim *et al.* [2008, 2010] computed the three-dimensional drift trajectories of relativistic electrons for various pitch angles under different solar wind conditions. They found that for all pitch angles, the last closed drift shell of the outer belt moves toward the Earth in response to large dynamic pressure increase and/or an intensification of the southward component of the IMF.

[6] As suggested by previous simulation studies, close correlations between the last closed drift shell distance and solar wind parameters could be identified if the MPS contributed to electron loss from the outer part of the outer belt. Most previous studies, however, have used the data only at geosynchronous orbit and were not able to directly determine the motion of the outer edge of the outer belt associated with the electron loss. Since THEMIS spacecraft can traverse the outer edge of the outer belt [Sibeck and Angelopoulos, 2008], the position of the outer edge can be identified. In this study, we first identify electron loss events at geosynchronous orbit using GOES data, and we then divide the loss events into two groups based on the extent of earthward movement of the outer edge as determined by THEMIS observations. We then investigate correlations between outer edge positions and solar wind parameters as well as the magnetopause standoff distance. Finally, we discuss the possible role of the MPS effect on electron loss at the outer part of the outer belt by comparing our results with test particle simulation results.

2. Data Analysis

[7] In this study, we use THEMIS-SST (Solid State Telescope) data [Angelopoulos, 2008]. The SST can measure electron and ion fluxes from ~ 30 keV to ~ 1 MeV. The SST electron channels used in this study are derived from the SST electron detector response to high-energy electrons. Ions are expected to be stopped in a ~ 4000 Å aluminum foil in front of the electron detector, but ions >400 keV will deposit measurable energy in the electron detector, and ions >1 MeV will contribute some flux to the >500 keV electron channels. Since the >1 MeV ion flux is typically well below the >500 keV electron flux at $L > 4$ (the region of interest in this study), proton contamination does not affect our results. Additionally, because the front electron detector is thin (300 microns), electrons >350 keV do not deposit their full energy in it. However, a good correlation between higher-energy electrons and the energy deposited in the front detector volume has been established by Ni *et al.* [2011]. In that work they compared the THEMIS data with LANL measurements and derived calibration factors for the THEMIS SST electron channels. To identify the dynamical variation of the outer radiation belt, we used a 12 h average of 422 keV, 655 keV, and 1.13 MeV electron flux data from THEMIS probe D (TH-D) from April 2007 to December 2008. The apogee altitude of TH-D is ~ 12 Re, and its orbital period is about 1 day. The magnetic local times of the

apogees are dawnside in spring, night side in summer, duskside in autumn, and dayside in winter.

[8] The analysis period (2007–2008) corresponds to solar minimum, so only a few magnetic storms occurred. Since many loss events are not associated with magnetic storms, we consider the contribution of the *Dst* effect to be relatively small. In this study, we use Roederer's L^* value (L^*), which is directly related to the third adiabatic invariant [Roederer, 1970] and maintains a constant value against adiabatic variations such as the *Dst* effect. Roederer's L^* value is estimated with the TS-05 storm magnetic field model [Tsyganenko and Sitnov, 2005]. The magnetopause standoff distance is derived from the Shue *et al.* [1997] model.

[9] We select events using the following criteria. First, we define the flux loss events at geosynchronous orbit using GOES measured MeV electron data with the same criteria as those of Ohtani *et al.* [2009]. Using the 1 day logarithmic average, Ohtani *et al.* [2009] defined the loss events with the following three conditions: (1) the 1 day average decreases at least by a factor of four; (2) the 90th percentile of electron flux during the subsequent 1 day interval is lower than that during the preceding 1 day interval at least by a factor of four; and (3) the 10th percentile of the electron flux during the 6 h interval is less than the half of the 10th percentile during the 6 h interval of the previous day when GOES was in the same local time sector. A 12 h interval for detecting the event corresponds to half the orbital period of TH-D. The number of events selected using this criterion is 110, 109, and 108 for energies of 422 keV, 655 keV, and 1.13 MeV, respectively. To identify the outer edge of the outer belt, we consider the location of 20% of the outer belt peak flux as a proxy for the outer edge L^* (L_p) for a 12 h interval. We confirmed similar results for the time variation of the outer edge with other percentages. To eliminate the contamination problem at small L^* , the peak L shell is identified only at $L^* \geq 4$. Note that if the flux data has data gaps between $L^* \geq 4$ and L_p in an interval, we do not use the interval to detect the outer edge of the outer belt. If there are multiple loss events within an interval, we select the event with the largest variation of L_p . After these THEMIS data reduction processes, we obtain 71 events for each energy channel.

[10] Next, we divide the above events into two groups, those with significant earthward movement of L_p and those without. To define significant earthward movement of L_p , we use the criterion that the outer edge moves earthward more than $0.3 L^*$ during each 12 h interval. Note that we changed this criterion from $0.1 L^*$ to $0.5 L^*$ and found that events with the criterion of more than $0.3 L^*$ showed a clear correlation with the magnetopause standoff distance.

[11] If THEMIS did not detect significant movement during an interval, the next interval is also used to find events. Therefore, we exclude the loss events that the edges are not found in two successive intervals. The number of loss events with (without) significant earthward movement of L_p for 422 keV, 655 keV, and 1.13 MeV is 32(9), 33(9), and 29(10), respectively. Outer edge variations often depend on electron energy, and we use only events in which the significant earthward movement of L_p can be identified in all three energy channels. Table 1 shows a list of events with significant earthward movement of L_p . The footnotes in

Table 1. Loss Events With Significant Earthward Movement of the Outer Edge of the Outer Belt

Event	Year/Month/Day	Day of Year
Event 1 ^a	2007/07/11	162
Event 2	2007/07/20	201
Event 3	2007/08/25	239
Event 4	2007/09/01	244
Event 5	2007/09/15	258
Event 6 ^b	2007/09/21	264
Event 7	2007/10/25	298
Event 8	2007/10/29	302
Event 9	2007/11/04	308
Event 10	2007/11/13	317
Event 11 ^a	2007/11/20	324
Event 12	2007/12/17	351
Event 13	2008/01/12	21
Event 14	2008/01/31	31
Event 15	2008/02/18	49
Event 16	2008/02/28	59
Event 17	2008/03/05	65
Event 18	2008/03/26	86
Event 19	2008/04/16	107
Event 20	2008/06/06	158
Event 21	2008/06/25	177
Event 22	2008/07/05	187
Event 23	2008/07/11	193
Event 24	2008/07/21	203
Event 25	2008/07/27	209
Event 26	2008/08/14	227
Event 27	2008/09/15	259
Event 28	2008/09/22	266
Event 29	2008/11/07	312
Event 30	2008/11/15	320
Event 31 ^a	2008/11/25	330
Event 32 ^a	2008/12/03	338
Event 33	2008/12/16	351

^aThe outer edge cannot be detected for 1.13 MeV due to the data gap.

^bThe outer edge cannot be detected for 422 keV due to the data gap.

Table 1 indicate that the outer edge cannot be detected for 422 keV and for 1.13 MeV.

3. Results

[12] Figure 1 shows the L -time diagram for 422 keV, 655 keV, and 1.13 MeV electron flux detected by THEMIS, >2 MeV electron flux measured by the GOES 11 satellite, the solar wind dynamic pressure and the solar wind IMF B_z by the OMNI-2 database, and the Dst index from August to October 2008. The red diamonds in the L -time diagram indicate loss events with significant earthward movement; the black diamonds correspond to loss events without significant earthward movement. The empirical magnetopause distance and L_p are shown in red and black lines, respectively.

[13] Around day of year (DOY) 227 and 259 indicated by the solid lines in Figure 1 (events 26 and 27 in Table 1), a clear decrease in MeV electrons can be seen at geosynchronous orbit (fourth panel of Figure 1). These two events are examples of loss events with significant earthward movement. During these events, the magnetopause moves earthward, the solar wind dynamic pressure has large value, and the IMF B_z shows the southward direction. For event 27, the dynamic pressure is 10.1 nPa, the IMF B_z is -5.5 nT, and the estimated magnetopause standoff distance is 7.8 Re. For event 26, the dynamic pressure is 2.3 nPa, IMF B_z is -4.3 nT, and the estimated magnetopause standoff distance is 9.8 Re.

The dynamic pressure and southward IMF of event 27 are larger than those of event 26, and the magnetopause of event 27 is closer to the Earth than that of event 26. L_p of event 27 is smaller than that of event 26. These findings are consistent with the simulation result of *Kim et al.* [2008]; L_p depends on the amplitude of the solar wind dynamic pressure and the southward IMF. If only adiabatic variation takes place, the ratio of the pre-event electron flux to the postevent electron flux should be the same as the ratio of the ambient magnetic field variations at the same L^* [*Kim and Chan*, 1997]. We found that the ratio of the differential flux is always larger than that of the ambient magnetic field at $L_p + 0.5$, consequently the observed loss is caused by nonadiabatic processes.

[14] Events around DOY 222 and 247 indicated by the dashed lines in Figure 1 are examples of the loss events without significant earthward movement. During these events, MeV electron flux decreases gradually inside geosynchronous orbit, as shown in the THEMIS observations, and relativistic electron flux is enhanced more than that of the previous day. If the electron flux enhancement occurs simultaneously with the loss during an interval, earthward movement of L_p is not expected to be clearly detected in this analysis. Therefore, some loss events without significant earthward movement may result from competition between flux enhancement and its decrease. Since we define L_p where the flux decreases by more than 20% relative to the peak as the outer edge, we do not recognize earthward movement of the outer edge if a similar radial profile of the flux is maintained.

[15] We then statistically examined the solar wind parameter dependence of loss events. Figure 2 shows the distribution of the occurrence ratio on the solar wind dynamic pressure and IMF B_z for the loss events at geosynchronous orbit. We derive the occurrence ratio from the number of count of each bins divided by that of the maximum count bin. The red color indicates distribution of loss events; black indicates the distribution for the entire period of this analysis. For Figure 2, we used the maximum dynamic pressure and the southward IMF during a 24 h interval around each event. In Figure 2a, the average of the dynamic pressure is 5.9 nPa for the loss events, whereas it is 2.0 nPa for the entire period. Therefore, the solar wind dynamic pressure for the loss events is higher than that for the usual solar wind. In Figure 2b, the average IMF B_z is -5.3 nT for the loss events, whereas it is -1.4 nT for the entire period. The IMF B_z for the loss events tends to be more southward than on average. A statistical test confirmed the significance of the difference between during these loss events and during the entire period. This is consistent with the statistical results of *Ohtani et al.* [2009]. We also obtained the similar solar wind parameter dependence with both loss events with/without significant movements.

[16] Next, we investigated the relationship between L_p and the magnetopause standoff distance. Figure 3 shows the results of the correlation analysis between the magnetopause standoff distance and L_p of the loss events with significant earthward movement. Figures 3a–3c correspond to the energies of 422 keV, 655 keV, and 1.13 MeV, respectively. Since the peak L shell of the outer belt depends on the electron energy [e.g., *Walt*, 1994], it is natural that L_p also depends on the electron energy in this analysis. It was found that L_p shifts earthward when the magnetopause moves closer to the Earth.

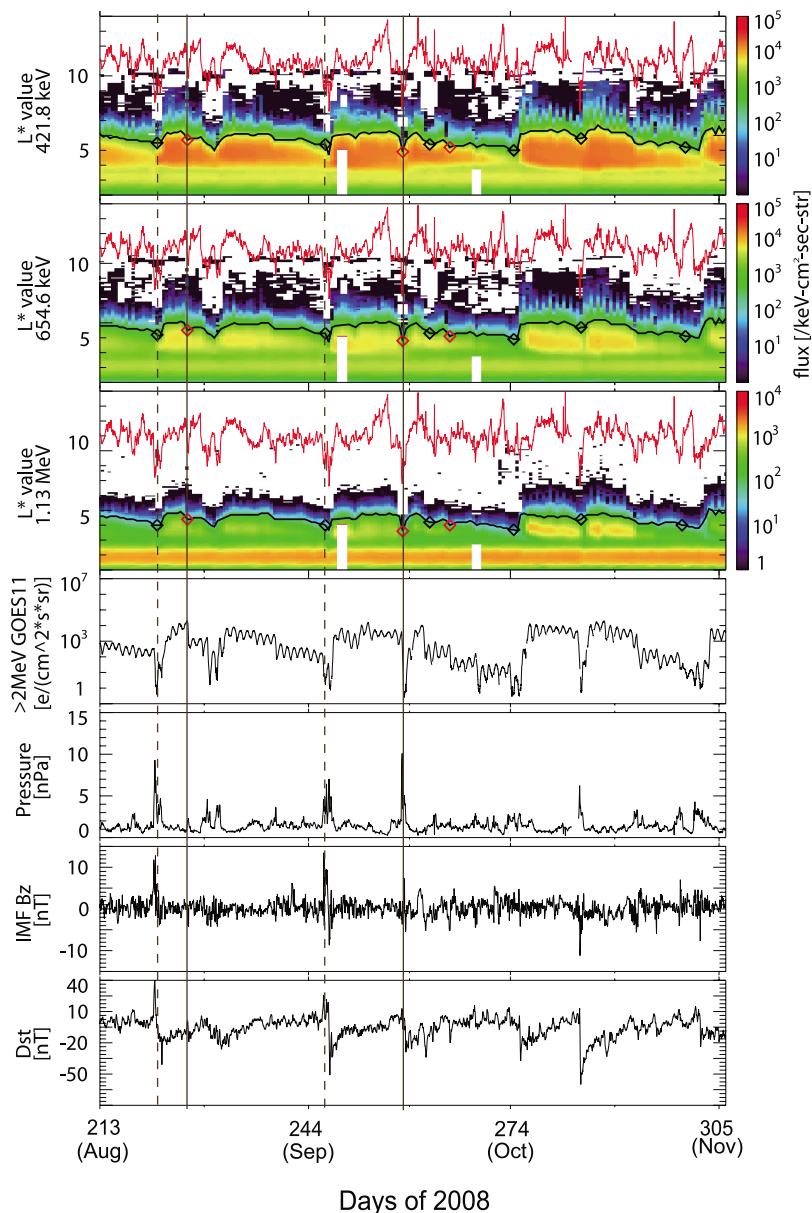


Figure 1. L -time diagram for 422 keV, 655 keV, and 1.13 MeV of the THEMIS/SST, GOES 11 > 2 MeV electron flux, solar wind dynamic pressure, solar wind IMF B_z , and Dst index from August to November 2008. The red and black diamonds in the L time diagram indicate events with the significant earthward L_p movement and events without significant movement, respectively. The empirical magnetopause distance and L_p are shown by red and black lines, respectively.

The correlation coefficients are 0.72, 0.76, and 0.70 for 422 keV, 655 keV, and 1.13 MeV, respectively, and are almost the same for the three energies. On the other hand, it seems that there is no clear correlation between magnetopause standoff distance and L_p for loss events without significant earthward movement (figure not shown).

4. Summary and Discussion

[17] In this study, we investigated electron loss events of the outer radiation belt in consideration of the earthward movement of L_p using GOES and THEMIS data. During the

electron loss events at geosynchronous orbit, both the dynamic pressure and the southward IMF tended to have larger values in comparison to that of usual solar wind. This result is consistent with that of *Ohtani et al.* [2009]. There is a good correlation between L_p and the magnetopause standoff distance in the loss events with significant earthward movement of L_p , but weak correlation in the events without significant earthward movement. These correlations can be seen in all energies from 422 keV to 1.13 MeV.

[18] As expected from simulation studies [e.g., *Kim et al.*, 2008], the correlation between L_p and the magnetopause standoff distance suggests that the MPS causes the loss of

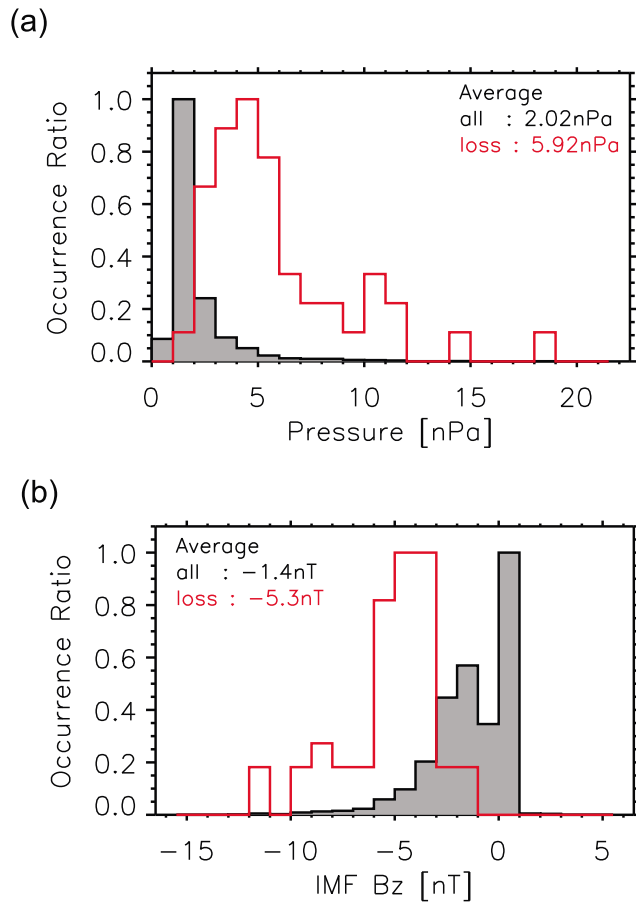


Figure 2. Occurrence ratios of (a) the solar wind dynamic pressure and (b) the IMF B_z . The red line corresponds to electron loss events at geosynchronous orbit, while the black line corresponds to the entire period.

energetic electrons at the outer part of the outer belt. To clarify whether the MPS causes the observed relationship between the magnetopause standoff distance and L_p , we compared the results of Figure 3 with those of the numerical simulation. We used the GEMSIS-RB code [Saito *et al.*, 2010] which was developed to calculate three-dimensional trajectories of relativistic electrons in the outer radiation belt with the TS-05 realistic magnetic field model. For this comparison, we changed the solar wind dynamic pressure and the IMF B_z with the constant Dst of 0 nT for the inputs of the simulation. The last closed drift shell of energetic electrons identified in the GEMSIS-RB code was used for the outer edge of the outer belt.

[19] Figure 4 shows the result of a comparison with the GEMSIS-RB simulation. Simulation results are presented for two different pitch angles (90° and 50°) as examples. The observational result shows that L_p shifts to the Earth when the magnetopause moves toward the Earth. A similar tendency can also be seen in the simulation. Since the present GEMSIS-RB does not include any loss mechanisms except for the MPS, the result shows that the MPS can cause the earthward shift of the outer edge associated with movement of the magnetopause standoff distance. Note that L_p is not the exact outer edge position of the outer belt but a proxy of the outer edge. The comparison with the GEMSIS-

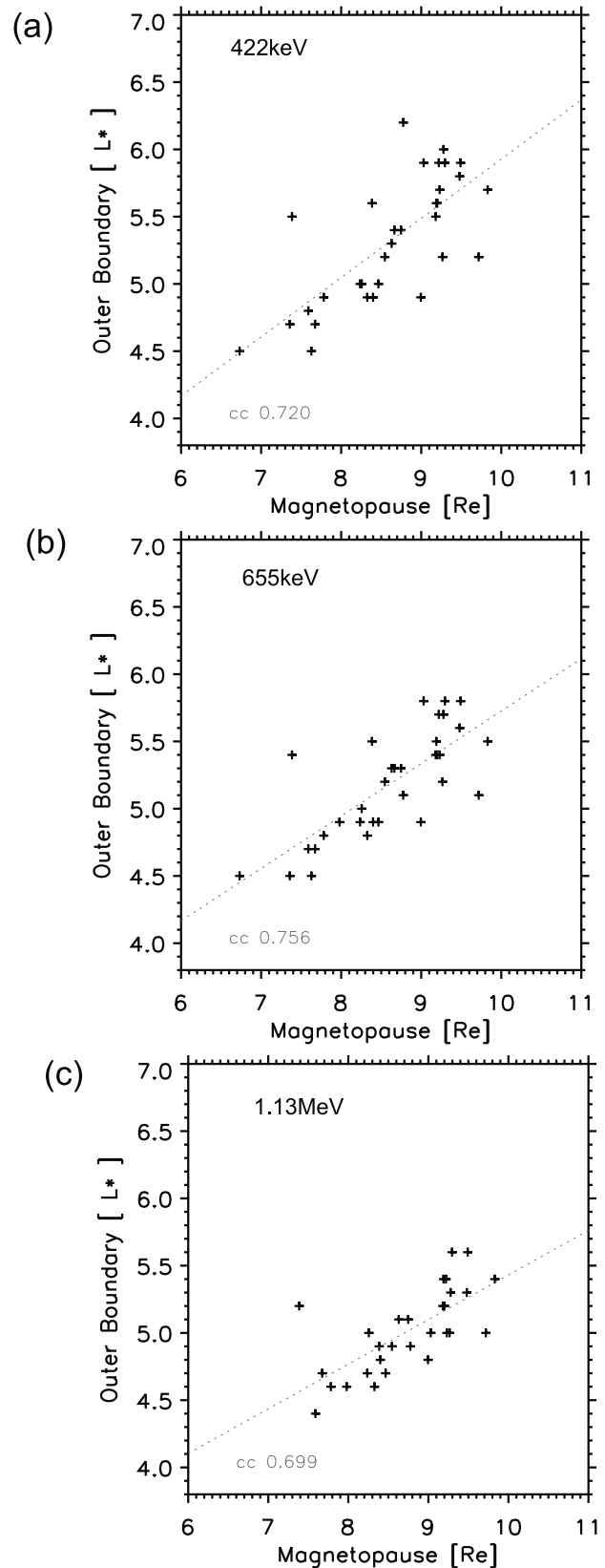


Figure 3. Relationship between L_p and the magnetopause standoff distance for the loss events with significant earthward movement of L_p : (a–c) 422 keV, 655 keV, and 1.13 MeV, respectively.

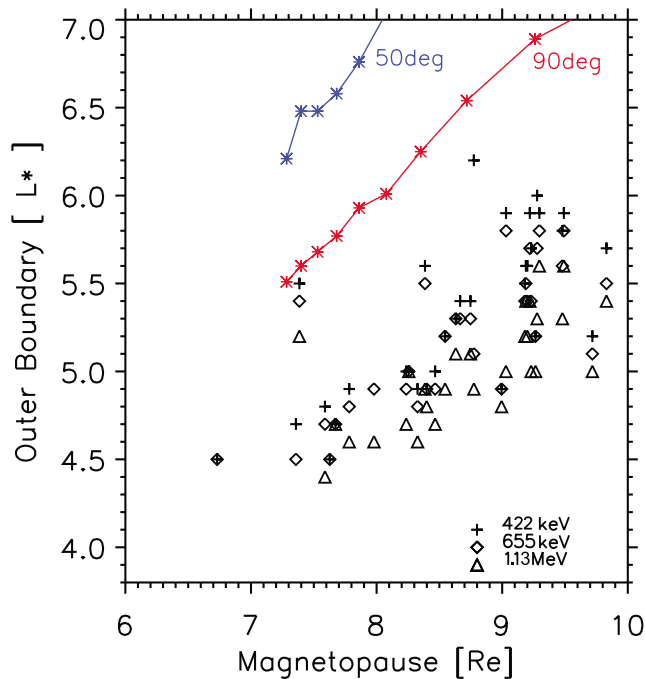


Figure 4. Magnetopause standoff distance dependence of L_p from observations and the last-closed drift L^* from the simulation. The red and blue lines correspond to the simulation results for the pitch angles of 90° and 50° , respectively.

RB code implies that the MPS explains the observed relationship between L_p and magnetopause standoff distance, and this suggests that the MPS is effective for the loss of the outer part of the outer belt.

[20] Green *et al.* [2004] suggested that the MPS cannot explain the flux dropouts because outer belt flux loss occurs far from the magnetopause. As shown in Figure 1, electron loss occurs over a wide range L shell inside the magnetopause. If the MPS takes place, the phase space density near the outer boundary would decrease sharply, inducing outward diffusion due to the negative phase space density gradient toward the magnetopause. Some simulation studies have shown that outward diffusion can cause reduction of relativistic electron flux in the heart of the outer radiation belt [Brautigam and Albert, 2000; Miyoshi *et al.*, 2003, 2006; Shprits and Thorne, 2004; Shprits *et al.*, 2006; Jordanova *et al.*, 2008]. Using THEMIS and GOES satellite observations as well as ground CARISMA magnetometer data, Loto'aniu *et al.* [2010] suggested that the combination of the MPS induced by the magnetopause compression and the outward diffusion causes the loss of the outer belt. If outward diffusion occurs after the MPS, the outer edge of the outer belt will be distributed in the wide L shell inside the open-closed drift shell.

[21] Onsager *et al.* [2007] showed that IMF B_z and solar wind dynamic pressure are correlated with loss of the outer radiation belt. Lyatsky and Khazanov [2008] suggested that the enhanced solar wind density is important to suppress electron flux enhancement at geosynchronous orbit. The solar wind parameter dependencies obtained in this study, which suggest that the MPS causes the loss of the outer belt, are consistent with the solar wind parameter dependencies of

electron loss about the IMF B_z and the solar wind dynamic pressure. Several other loss mechanisms may have similar parameter dependences, however. Some previous studies suggest that different loss processes work simultaneously at different radial distances and local times [e.g., Bortnik *et al.*, 2006; Millan *et al.*, 2010; Morley *et al.*, 2010]. For future studies, a more detailed survey using THEMIS multipoint observations is necessary to better understand the variety of the loss processes at different locations.

[22] **Acknowledgments.** We thank S. Ohtani for valuable discussions. The OMNI-2 solar wind and geomagnetic index data were provided by NASA/NSSDC and WDC-C2, Kyoto University, respectively. This work has been supported by the Japan Society for the Promotion of Science (JSPS) Grants-in-Aid for Young Scientists B (20740283) and JSPS Grant-in-Aid for Scientific Research (Category B, 20340134).

[23] Masaki Fujimoto thanks the reviewers for their assistance in evaluating this paper.

References

- Angelopoulos, V. (2008), The THEMIS mission, *Space Sci. Rev.*, *141*, 5–34, doi:10.1007/s11214-008-9336-1.
- Borovsky, J. E., and M. H. Denton (2009), Relativistic-electron dropouts and recovery: A superposed epoch study of the magnetosphere and the solar wind, *J. Geophys. Res.*, *114*, A02201, doi:10.1029/2008JA013128.
- Bortnik, J., R. M. Thorne, T. P. O'Brien, J. C. Green, R. J. Strangeway, Y. Y. Shprits, and D. N. Baker (2006), Observation of two distinct, rapid loss mechanisms during the 20 November 2003 radiation belt dropout event, *J. Geophys. Res.*, *111*, A12216, doi:10.1029/2006JA011802.
- Brautigam, D., and J. Albert (2000), Radial diffusion analysis of outer radiation belt electrons during the October 9, 1990, magnetic storm, *J. Geophys. Res.*, *105*, 291–309, doi:10.1029/1999JA900344.
- Green, J. C., T. G. Onsager, T. P. O'Brien, and D. N. Baker (2004), Testing loss mechanisms capable of rapidly depleting, *J. Geophys. Res.*, *109*, A12211, doi:10.1029/2004JA010579.
- Jordanova, V. K., J. Albert, and Y. Miyoshi (2008), Relativistic electron precipitation by EMIC waves from self-consistent global simulations, *J. Geophys. Res.*, *113*, A00A10, doi:10.1029/2008JA013239.
- Kim, H.-J., and A. Chan (1997), Fully adiabatic changes in storm time relativistic electron fluxes, *J. Geophys. Res.*, *102*, 22,107–22,116.
- Kim, H.-J., K. C. Kim, D.-Y. Lee, and G. Rostoker (2006), Origin of geosynchronous relativistic electron events, *J. Geophys. Res.*, *111*, A03208, doi:10.1029/2005JA011469.
- Kim, K. C., D.-Y. Lee, H.-J. Kim, L. R. Lyons, E. S. Lee, M. K. Öztürk, and C. R. Choi (2008), Numerical calculations of relativistic electron drift loss effect, *J. Geophys. Res.*, *113*, A09212, doi:10.1029/2007JA013011.
- Kim, K. C., D.-Y. Lee, H.-J. Kim, E. S. Lee, and C. R. Choi (2010), Numerical estimates of drift loss and Dst effect for outer radiation belt relativistic electrons with arbitrary pitch angle, *J. Geophys. Res.*, *115*, A03208, doi:10.1029/2009JA014523.
- Li, W., Y. Y. Shprits, and R. M. Thorne (2007), Dynamic evolution of energetic outer zone electrons due to wave-particle interactions during storms, *J. Geophys. Res.*, *112*, A10220, doi:10.1029/2007JA012368.
- Loto'aniu, T. M., H. J. Singer, C. L. Waters, V. Angelopoulos, I. R. Mann, S. R. Elkington, and J. W. Bonnell (2010), Relativistic electron loss due to ultralow frequency waves and enhanced outward radial diffusion, *J. Geophys. Res.*, *115*, A12245, doi:10.1029/2010JA015755.
- Lyatsky, W., and G. V. Khazanov (2008), Effect of solar wind density on relativistic electrons at geosynchronous orbit, *Geophys. Res. Lett.*, *35*, L03109, doi:10.1029/2007GL032524.
- Lyons, L. R., R. M. Thorne, and C. F. Kennel (1972), Pitch-angle diffusion of radiation belt electrons within the plasmasphere, *J. Geophys. Res.*, *77*, 3455–3474.
- Millan, R. M., and R. M. Thorne (2007), Review of radiation belt relativistic electron losses, *J. Atmos. Sol. Terr. Phys.*, *69*, 362–377.
- Millan, R. M., K. B. Yando, J. C. Green, and A. Y. Ukhorskiy (2010), Spatial distribution of relativistic electron precipitation during a radiation belt depletion event, *Geophys. Res. Lett.*, *37*, L20103, doi:10.1029/2010GL044919.
- Miyoshi, Y., and R. Kataoka (2005), Ring current ions and radiation belt electrons during geomagnetic storms driven by coronal mass ejections and corotating interaction regions, *Geophys. Res. Lett.*, *32*, L21105, doi:10.1029/2005GL024590.

- Miyoshi, Y., and R. Kataoka (2011), Solar cycle variations of outer radiation belt and its relationship to solar wind structure dependence, *J. Atmos. Sol. Terr. Phys.*, *73*, 77–87.
- Miyoshi, Y., A. Morioka, T. Obara, H. Misawa, T. Nagai, and Y. Kasahara (2003), Rebuilding process of the outer radiation belt during the 3 November 1993 magnetic storm: NOAA and Exos-D observations, *J. Geophys. Res.*, *108*(A1), 1004, doi:10.1029/2001JA007542.
- Miyoshi, Y. S., V. K. Jordanova, A. Morioka, M. F. Thomsen, G. D. Reeves, D. S. Evans, and J. C. Green (2006), Observations and modeling of energetic electron dynamics during the October 2001 storm, *J. Geophys. Res.*, *111*, A11S02, doi:10.1029/2005JA011351.
- Miyoshi, Y., K. Sakaguchi, K. Shiokawa, D. Evans, J. Albert, M. Connors, and V. Jordanova (2008), Precipitation of radiation belt electrons by EMIC waves, observed from ground and space, *Geophys. Res. Lett.*, *35*, L23101, doi:10.1029/2008GL035727.
- Morley, S. K., R. H. W. Friedel, T. E. Cayton, and E. Noveroske (2010), A rapid, global and prolonged electron radiation belt dropout observed with global positioning system constellation, *Geophys. Res. Lett.*, *37*, L06102, doi:10.1029/2010GL042772.
- Nagai, T. (1988), “Space weather forecast”: Prediction of relativistic electron intensity at synchronous orbit, *Geophys. Res. Lett.*, *15*(5), 425–428.
- Ni, B., Y. Shprits, M. Hartinger, V. Angelopoulos, X. Gu, and D. Larson (2011), Analysis of radiation belt energetic electron phase space density using THEMIS SST measurements: Cross-satellite calibration and a case study, *J. Geophys. Res.*, *116*, A03208, doi:10.1029/2010JA016104.
- O’Brien, T. P., M. D. Looper, and J. B. Blake (2004), Quantification of relativistic electron microburst losses during the GEM storms, *Geophys. Res. Lett.*, *31*, L04802, doi:10.1029/2003GL018621.
- Ohtani, S., Y. Miyoshi, H. J. Singer, and J. M. Weygand (2009), On the loss of relativistic electrons at geosynchronous altitude: Its dependence on magnetic configurations and external conditions, *J. Geophys. Res.*, *114*, A01202, doi:10.1029/2008JA013391.
- Onsager, T. G., G. Rostoker, H.-J. Kim, G. D. Reeves, T. Obara, H. J. Singer, and C. Smithro (2002), Radiation belt electron flux dropouts: Local time, radial, and particle-energy dependence, *J. Geophys. Res.*, *107*(A11), 1382, doi:10.1029/2001JA000187.
- Onsager, T. G., J. C. Green, G. D. Reeves, and H. J. Singer (2007), Solar wind and magnetospheric conditions leading to the abrupt loss of outer radiation belt electrons, *J. Geophys. Res.*, *112*, A01202, doi:10.1029/2006JA011708.
- Reeves, G. D., K. L. McAdams, R. H. W. Friedel, and T. P. O’Brien (2003), Acceleration and loss of relativistic electrons during geomagnetic storms, *Geophys. Res. Lett.*, *30*(10), 1529, doi:10.1029/2002GL016513.
- Roederer, J. G. (1970), *Dynamics of Geomagnetically Trapped Radiation*, Springer, Berlin.
- Saito, S., Y. Miyoshi, and K. Seki (2010), A split in the outer radiation belt by magnetopause shadowing: Test particle simulations, *J. Geophys. Res.*, *115*, A08210, doi:10.1029/2009JA014738.
- Shprits, Y. Y., and R. M. Thorne (2004), Time dependent radial diffusion modeling of relativistic electrons with realistic loss rates, *Geophys. Res. Lett.*, *31*, L08805, doi:10.1029/2004GL019591.
- Shprits, Y. Y., R. M. Thorne, R. Friedel, G. D. Reeves, J. Fennell, D. N. Baker, and S. G. Kanekal (2006), Outward radial diffusion driven by losses at magnetopause, *J. Geophys. Res.*, *111*, A11214, doi:10.1029/2006JA011657.
- Shue, J.-H., J. K. Chao, H. C. Fu, C. T. Russell, P. Song, K. K. Khurana, and H. J. Singer (1997), A new function form to study the solar wind control of the magnetopause size and shape, *J. Geophys. Res.*, *102*, 9497–9511.
- Sibeck, D. G., and V. Angelopoulos (2008), THEMIS science objectives and mission phases, *Space Sci. Rev.*, *141*, 35–59, doi:10.1007/s11214-008-9393-5.
- Tsyganenko, N. A., and M. I. Sitnov (2005), Modeling the dynamics of the inner magnetosphere during strong geomagnetic storms, *J. Geophys. Res.*, *110*, A03208, doi:10.1029/2004JA010798.
- Ukhorskiy, A. Y., B. J. Anderson, P. C. Brandt, and N. A. Tsyganenko (2006), Storm time evolution of the outer radiation belt: Transport and losses, *J. Geophys. Res.*, *111*, A11S03, doi:10.1029/2006JA011690.
- Walt, M. (1994), *Introduction to Geomagnetically Trapped Radiation*, Cambridge Univ. Press, Cambridge, U. K.
- V. Angelopoulos, IGPP, University of California, Los Angeles, CA 90095, USA.
- J. Koller, Los Alamos National Laboratory, PO Box 1663, MS D466, Los Alamos, NM 87545, USA.
- C. Matsumura, Y. Miyoshi, and K. Seki, Solar-Terrestrial Environment Laboratory, Nagoya University, Nagoya 464-8601, Japan. (miyoshi@stelab.nagoya-u.ac.jp)
- S. Saito, National Institute of Information and Communications Technology, 4-2-1 Nukui-Kitamachi, Koganei 184-8795, Japan.